The impact of climate change on barley yield in the Mediterranean basin

Davide Cammarano[1,*], Salvatore Ceccarelli[2], Stefania Grando[3], Ignacio Romagosa[4], Abdelkader Benbelkacem[5], Tanek Akar[6], Adnan Al-Yassin[7], Nicola Pecchioni[8,9], Enrico Francia[9], Domenico Ronga[1,9,10].

[1]James Hutton Institute, Invergowrie, DD25DA, Scotland, U.K.

[2]Rete Semi Rurali, Italy.

[3]International Consultant.

[4]Agrotecnio Center, Universitat de Lleida, Spain.

[5]INRAA, Algeria.

[6]Akdeniz University Faculty of Agriculture, Dept. of Agronomy, Antalya, TURKIYE.

[7]Consultant and barley breeder, National Agricultural Research Center, Amman, Jordan.

[8] Council for Agricultural Research and Economics (CREA) Research Centre for Cereal and Industrial Crops (CREA-CI), S.S. 673 km 25,200, 71122 Foggia, Italy

[9]University of Modena and Reggio Emilia, Department of Life Sciences, Via G. Amendola 2, 42122 Reggio Emilia, Italy

[10]Council for Agricultural Research and Economics – Research Center for Animal Production and Aquaculture (CREA-ZA), Viale Piacenza, 29, 26900, Lodi, Italy.

Corresponding author: davide.cammarano@hutton.ac.uk;

Abstract

Barley is an important cereal crop for the arid and semi-arid Mediterranean environments. Future climate projections show that Mediterranean countries will get drier and hotter. The objectives of the study are to: i) simulate the impacts of different climate projections and different sowing dates on yield; ii) quantify the importance of heat and drought on barley yield at different growth stages and sowing dates; iii) quantify the contributions of sources of uncertainty among inter-annual variability, adaptation options and climate projections. Nine locations across the Mediterranean basin were used to calibrate and evaluate the Decision Support System for Agrotechnology Transfer (DSSAT) model. At each location the 40 Global Circulation Model (GCM) outputs (RCP4.5, Mid of the Century) showed an increase in mean growing season temperature between 0.9 and 2.16°C, while changes of growing season rainfall were between -24 and +24%. Therefore, at each location a drier (Dry), mid (Mid), and wetter (Wet) projection was selected. Overall, there was a 9% reduction in grain yield under climate change; but the mean yield change was -27%, +4%, +8%, for the Dry, Mid, and Wet scenarios, respectively. The results of the simulations under the Wet scenario showed a higher variability of yield response. There was an interaction between the soil type, the amount of rainfall, the extractable soil water content and the maximum air temperature. Because of these relationship water-stress during the vegetative stage was experienced, affecting expansive growth. At the same time, the high number of days with T_{max}>34°C caused higher soil water depletion by the plant and therefore lower yields under the Wet scenario. The inter-annual weather variability impacts barley yield irrespective of the sowing dates and the future projected climate. In conclusion, the impact of future climate on barley yield in the Mediterranean is negative but some locations will be less affected than others.

Keywords: Barley; Mediterranean environment; Climate change; Soil water content; drought; Heat; Climate extremes.

1. Introduction

Barley is an important cereal crop for the arid and semi-arid Mediterranean environments. It is cultivated from the equator to the Arctic Circle and at different elevations (Ceccarelli et al., 2011; Dawson et al., 2015). Europe produces about 63% of the world's barley with most of it under rainfed conditions (FAOSTAT, 2018). Evidence suggests that cereals crop yield is peaking worldwide, and barley yields in Mediterranean countries follow the same trend (Martre et al., 2015; Dawson et al., 2015). Mediterranean environments are characterised by hot dry summers and humid, cool winters with high variability in patterns of rainfall and temperature impacting yield gains (Brisson et al., 2010).

Future projections of climate trends show that Mediterranean countries will get drier and hotter and might result in severe yield reduction (Semenov et al., 2014; Senapati et al., 2018). During reproductive development, both heat and drought have negative effects on final yield (Semenov et al., 2014; Asseng et al., 2015). However, both factors are part of the soil-plant-atmosphere system and they dynamically interact within such system. Mean air temperature is the main driver of canopy and leaf temperature, affecting photosynthetic rates, and higher temperatures will negatively influence yield by damaging reproductive organs and accelerating senescence rates (Asseng et al., 2011). Soil moisture limitation will have negative impacts on crop expansive growth and regulating leaves' stomatal conductance (Huntingford et al., 2005). When soil water contents and mean air temperature are not limiting both photosynthesis and transpiration at leaf's level will occur at normal rates (Saseendran et al., 2008). At higher air temperatures and low vapour pressure deficit (VPD) plants open the stomata to avoid heat stress, increasing the inter-cellular CO_2 concentration and biomass growth. When soil water content is the limiting factor the stomata are closed, causing dissection, negative impact on photosynthesis, low intercellular CO_2 concentration and therefore lower biomass (Kobza and Edwards, 1987). In addition, in Mediterranean

environments, where crops rely on soil moisture stored prior sowing, an adequate level of soil available water content is vital to achieve certain yield levels. Therefore, the patterns of rainfall prior sowing will also be an important determinant of crop yield (Passioura, 2006).

To explore the impacts of climate variability and changes on grain production, crop simulation models (CM) are generally used. They simulate daily growth, development, and yield as influenced by daily weather, soil type, crop features and agronomic management (Cammarano and Tian, 2018). The rationale of using CM to explore the climate impacts is because they can extrapolate the daily interactions of soil water and nutrient beyond one single growing season (Jones et al., 2003). In addition to the use of CM, Global Climate Models (GCM) provide the atmospheric input of climate projections to such models.

A combination of data and modelling results have been used to explore the impact of environmental condition on crop production (O'Leary et al., 2015; Rötter et al., 2012). An ensemble of 30 wheat crop models was tested against field experimentations and at different locations worldwide, the application of such ensemble showed that global wheat production will fall by 6% for each °C of temperature increase (Asseng et al., 2015). Overall, on many crops important for food security (e.g. cereal, legumes, sugarcane) even a moderate increase in air temperature will likely have a major negative impact if no adaptation measures are taken. It is expected that negative impacts will be more relevant in developing countries (Rosenzweig et al., 2014; Lobell et al., 2008; Challinor et al., 2014; Porter et al., 2014). Therefore, adaptation options are the best option for maintaining future food needs. Challinor et al. (2014) and Porter et al. (2014) concluded that adaptation options could help to increase mean yield by about 7% regardless of the warming levels. In a recent study it was found that global barley yields will decline between 3 to 17%, depending on the geographical location, and in many areas of North Africa, the horn of Africa and South America (where it is an

important food crop) the negative projected yield changes will impact food security (Grando et al., 2005; Xie et al., 2018).

Recent scientific efforts using CM focused on the effect of heat stress on development and yield (Asseng et al., 2016; Asseng et al., 2015). Xie et al. (2018) studied the impacts of climate extremes on global barley yields, focusing on drought and heat stresses. However, there are, to the best of our knowledge, virtually no simulation studies on barley specific for the Mediterranean conditions where the impacts of projected changes of heat and drought on barley is explored; as well as the impact of agronomic adaptation options. Tao et al. (2018) developed a triple-ensemble probabilistic assessment by using a combination of CMs, model parameters, and climate projections to find the main source of uncertainty. The study did not focus on the impacts of climate change on barley per-se but helped to quantify that the major uncertainty was in the models' structure rather than the climate projections.

We hypothesize that, depending on the climate projection (e.g. drier or wetter), the impacts of changing agronomic practices might offset the negative impacts of climate change. In addition, the importance of future drought and heat stresses on barley yield will be explored prior sowing, at vegetative and reproductive stages. Finally, the sources of uncertainty coming from inter-annual climatic variability, adaptation strategy, and climate scenario were analysed. The objectives of the study are to: i) simulate the impacts of different climate projections and different sowing dates on yield; ii) quantify the importance of heat and drought on barley yield at different growth stages and prior sowing; iii) quantify the contributions of sources of uncertainty among inter-annual variability, adaptation options and climate projections.

2. Materials and Methods

2.1.Study area

The study area comprises the Mediterranean basin; nine locations spanning from Northern Africa to Southern Europe were selected because data were available from a study of Francia et al. (2011), where several genotypes were tested in these locations for three years (2003, 2004, and 2005). No remarkable incidence of biotic stresses was recorded at any site. During the three years, two locations had additional irrigation and all the others were rainfed. The geographical distribution of the locations is shown in Figure 1. Information regarding the sowing, anthesis, maturity and yield were available in Francia et al. (2011). In addition, information on the soil water holding capacity were also available, and the co-authors of that study provided information regarding the soil texture and organic carbon levels.

2.2.Weather data

One growing season of daily weather data was available at each site. Daily values of solar radiation (MJ m^{-2} d^{-1}), maximum temperature (°C), minimum temperature (°C), and rainfall (mm) were used. To have a long-term weather data series, needed as baseline for our study, the daily data at each location were reconstructed for the period 1980-2010 using the NASA AgMERRA product (Ruane et al., 2015). Such dataset has been used in many climate change impact studies worldwide (Rosenzweig and Hilell, 2015; Elliot et al., 2015). To quantify the quality of the constructed time series the observed year of weather data was compared against the NASA AgMERRA.

2.3.Climate projections

The climate projections were obtained using the global Coupled Model Intercomparison Project Phase 5 (CMIP5) data for temperature, precipitation, and solar radiation (Taylor et al., 2012). To generate perturbed daily weather data, the DSSAT-Perturb software was used

(ClimSystem, 2018). The software used the baseline weather data at each location, and by integrating the CMIP5 from 40 Global Circulation Models (GCM; Tab. A1), generates projected daily weather data. More details about algorithms behind the software are found in Yin et al. (2013). At each location, the future daily output of 40 GCMs were produced at a Representative Concentration Pathway 4.5 (RCP 4.5) Mid of the Century (Tab. A2). At each location, the percentage change in terms of growing season rainfall and temperature with respect to the baseline was calculated for each GCM. Then, a similar approach detailed in the study of Ruane and McDermid (2017) for each location was chosen to pick 3 site-specific GCMs. But, to narrow down the number of GCMs chosen, at each location three GCMs were selected. They were selected to provide similar amount of growing season temperature increase but "drier", "little" and "wetter" changes of rainfall with respect to the baseline.

2.4.*Crop simulation*

The DSSAT v4.7 was used for this study (Decision Support System for Agrotechnology Transfer), the CERES-Barley model was the crop-specific used (Jones et al., 2003; Hoogenboom et al., 2010). The input data for the model were the ones obtained at each experimental site, and a generic barley cultivar was calibrated (Tab. A3) using the observations reported in Table 1 in the study of Francia et al. (2011). The initial soil water and nitrogen content, known as "initial conditions", are two important parameters determining the quality of the simulation runs. In this study, the date of the initial conditions (when the crop model started running) were assumed to be after the generic harvest date for each location. Therefore, this allowed to start with a relatively dry soil profile (10% above the soil Lower Limit), while for the initial nitrogen in the soil experts' opinion from agronomists from each site were used. The nitrogen fertilizer management was also derived from experts' opinion and from local researchers at each location. The crop model was calibrated using the two irrigated sites and evaluated on the remaining sites.

169 The sowing dates used for the simulations ranged from mid-September to mid-January
170 (sowing happening every 15 days; S1 to S8) at each location and were run for the baseline
171 and for each of the 3 scenarios. The atmospheric CO_2 concentration used by the model for the
172 baseline runs (1980-2010) was 360ppm while at RCP4.5 it was 499ppm. The model's runs
173 were set up to re-initialize every growing season. Every growing season the models started
174 with the same initial conditions, same sowing date, and same fertilizer management. The only
175 thing that changed was the weather conditions. In this way, the impacts of climate and
176 weather variability can be quantified.

177 2.5.*Statistical analysis*

178 The goodness of fit of the simulated vs. observed data for calibration and evaluation was
179 calculated using the Root Mean Square Error (RMSE) as follows:

180 $$RMSE = \sqrt{\frac{1}{n}\sum_{i=1}(y_i - \hat{y}_i)^2} \quad [1]$$

181 where y_i are the observations, $\hat{y}_i$ the simulations, and *n* is the number of comparisons. In
182 addition, the Wilmott index of agreement (D-Index) was calculated (Wilmott, 1982). The
183 index ranges from 0 (poor model) to 1 (good model). The index is a descriptive measure and
184 can be widely applied to make cross-comparison between models (Wilmott, 1982). It is
185 calculated as follows:

186 $$d - Index = 1 - \frac{\sum_{i=1}^{n}(y_i - \hat{y}_i)^2}{\sum_{i=1}^{n}(|y_i - \bar{y}| + |\hat{y}_i - \bar{y}|)^2} \quad [2]$$

187 Were $\bar{y}$ is the mean of the observed values. The relative grain yield change was calculated as:

188 $$RY = \frac{y_{future,k,i} - y_{baseline,i}}{y_{baseline,i}} * 100 \quad [3]$$

where $y_{future,i}$ is the simulated yield predicted by the GCM *k*, and for the growing season *i*, and $y_{baseline,i}$ is the baseline yield simulated for the growing season *i*. The box and whiskers plots show the distribution of responses for each growing season. The horizontal line represents the median, the box delimits the 25th and 75th percentiles, and the whiskers the 10th and 90th percentile, respectively.

From the start of simulation to the day of sowing (SP), from sowing to anthesis (PA), and from anthesis to maturity (AM) the delta (Δ) changes of rainfall and days of daily maximum temperature > 34°C (T_{max}>*34°C)* was calculated. This temperature threshold was chosen because it was linked to heat stress and yield reductions due to acceleration in senescence rates (Asseng et al., 2011). It was calculated as follows:

$$\Delta = RCP_{var,i} - Baseline_{var,i} \quad [4]$$

where $RCP_{var,i}$ is the variable under each of the scenario and each sowing time (*i*), and $Baseline_{var,i}$ is the variable under baseline conditions and each sowing time (*i*).

The extractable water content values for each location, each sowing and each climate scenario were calculated as Delta respect to the start of the simulation date.

$$\Delta Extractable\ water = ewc_d - ewc_s \quad [5]$$

ewc_d represents the extractable soil water content at either Planting (P), anthesis (A), Maturity (M) and ewc_s is the extractable soil water content at the start of simulation (S).

To calculate the magnitude of yield variability coming from the inter-annual baseline climate variability, future climatic variability, the sowing date and the three climate projections (Dry, Mid, Wet) the approach described in Asseng et al. (2013) was considered. For each location and at baseline, the variability across sowing date and within each sowing date (inter-annual variability) was calculated by computing the averages of yield. Then, the

212 standard deviation between years and between locations was computed. For each scenario,
213 the delta yield between baseline and future was calculated. Then the averages and standard
214 deviations between the scenarios and the sowing dates was calculated. Once all the average
215 and standard deviations were calculated the Coefficient of Variation was calculated for the
216 inter-annual variability, the Sowing-Baseline, Sowing-Future, and Scenarios. All the figures
217 were drawn using the library GGPLOT2 from the statistical package R (Wickham, 2016).

218

219 ## 3. Results

220 The calibration of the generic barley cultivar following the information presented on the
221 study of Francia et al. (2011) showed a good agreement between simulated and observed data
222 for both phenology and yield, with d-Index values always above 0.5 (Table 1). For the
223 evaluation of the model, not all the sites had the phenology information, and, when available
224 they were used. Overall, phenology was well simulated, with a RMSE of 6 and 10 days for
225 anthesis and maturity, respectively (Tab. 1). The observed yield values for the calibration and
226 evaluation dataset are reported in Supplemental Material (Table A4). Overall, the yields
227 under irrigated conditions did not vary too much, while under rainfed conditions observed
228 yields ranged between 70 kg DM ha^{-1} in Jordan to 5400 kg DM ha^{-1} in Syria (Table A4). The
229 simulated yields for the evaluation dataset showed that in some location's yields were under-
230 estimated. For example, in Jordan (JORB) yields were 70 kg DM ha^{-1} for the observed and
231 1439 kg DM ha^{-1} for the simulated one (Tab. A4).

232 The reconstructed long-term weather series using AgMERRA, when compared with the
233 observed growing season data showed good agreement between the data (Supplemental
234 Material Figs. 1-4). For solar radiation the RMSE was 3.7 MJ d^{-1} m^{-2} (Fig. A1), while for
235 daily maximum and minimum temperature it was 2.8 and 3.5°C, respectively (Figs. A2 and

236 A3). Growing season rainfall was compared by plotting the bar plots of the frequency of
237 rainfall at every 2mm intervals and a good agreement between the observed and the
238 AgMERRA data was found (Fig. A4).

239 The list of the 40 GCMs for the RCP4.5 Mid of the Century is shown in Supplemental
240 Table 1. At RCP4.5 all the GCM projected an average mean growing season temperature
241 increase between 7 and 18% (Tab. 2). On the other hand, the differences in changes in
242 growing season rainfall were rather large among GCMs. The overall range of coefficient of
243 variations of the growing season rainfall ranged between 108 and 380%. The three GCM at
244 each location were named as "Dry", "Mid", and "Wet" and had an overall growing season
245 rainfall change of -19%, 0.2%, and +18%, respectively (Tab. 2).

246 The mean growing season temperature was higher for GCMs with respect to the baseline
247 and among the 3 GCMs it was higher for the drier scenario; it increased for later sowing dates
248 at all location (Fig. A5). There was a degree of variability among locations, with Jordan and
249 Turkey showing the greatest variability of mean temperature, especially for the Dry scenario
250 (Fig. A5). Growing season rainfall showed higher variability than temperature even for the
251 baseline climate data. Some locations (e.g. Jordan-Ramtha, Spain and Turkey) had little
252 variability of growing season rainfall for any sowing dates, while others (e.g. Italy
253 Fiorenzuola) where rather variable (Fig. A6).

254 Simulated impacts of climate change on grain yield showed an overall mean yield change of
255 -27%, +4%, +8%, for the Dry, Mid, and Wet scenarios, respectively (Fig. 2). There was a
256 strong location effect with positive mean changes for all the scenarios at Italy-Fiorenzuola,
257 and with strong negative effects for all the scenarios at Jordan-Rabba (Fig. 2). The negative
258 impact of the Dry scenario was consistently high at Jordan-Ramtha with -65% simulated
259 yield. However, at the same location, the Wet scenario showed an overall increase of 25% of

grain yield (Fig. 2). The results of the simulations under the Wet scenario showed a higher variability of yield response at each sowing date. The impact of sowing dates on simulated yield depends on the scenario and location considered. Under the Dry scenario late sowings caused an overall 44% yield reduction with respect to early sowing, consistently reducing yield at each location (Fig. 2). On the other hand, under the Wet scenario there was an overall 50% increase of simulated yield with later sowing dates. There is less consistency among locations; for example, at Jordan-Rabba and Spain there was no yield benefit from later sowing (Fig. 2).

The impact of heat and drought on simulated grain yield is shown in Figure 3. The negative values of the Δ indicated that the values under baseline conditions were higher than the ones under the given scenario and the given crop stage. The amount of rainfall that fell before sowing (defined as the period from a generic harvest time and the sowing date and referred to as fallow rainfall) was -22, 2, and 25mm under the Dry, Mid, and Wet scenarios, respectively (Fig. 3a, red symbols). There was little response of yield changes as changes in fallow rainfall, except with the Wet scenario where at given increased of Δrain corresponded increases of Δyield (Fig. 3a; red squares). Between sowing to anthesis (PA, yellow symbols) the simulated yield under the dry scenario showed negative responses to changes in rainfall during the vegetative stage. There was a change from -13 to -100 mm of rainfall during this stage across the locations and sowing dates, and this showed a decline in yield between -49 to -1351 kg DM ha^{-1} (Fig. 3a). From anthesis to maturity (AM; green symbols) there were little changes in rainfall which might not be cause of the changes in simulated yields (Fig. 3a). The Δ number of days of T_{max}>34°C was higher for the Dry scenarios at SP, PA, and AM (Fig. 3b). The Δyield under the Wet scenario ranged between -259 to 845 kg DM ha^{-1} (Fig. 3b). The number of days of T_{max}>34°C was between 6 to 24 days, and 0 and 15 days, at SP and PA across the GCMs, respectively (Fig. 3b). The main difference was between AM when the

285 number of days of T_{max}>34°C diverged between the Dry and Wet scenarios, with the former
286 showing on average 5 additional days of T_{max}>34°C (Fig. 3b).

287 At reproductive stage, the number of days of T_{max}>34°C showed a strong location effect and
288 degrees of variability for each sowing date (Fig. 4). When simulations were run under
289 baseline weather, the average number of days of T_{max}>34°C ranged across locations between
290 0 and 20. Later sowing dates showed the highest number of days of T_{max}>34°C (Fig. 4). The
291 inter-annual variability, represented by the individual boxplot, did not differ too much within
292 and across locations. One location, Italy Fiorenzuola, did not have any day of T_{max}>34°C,
293 while a location like Syria-Breda showed the highest number of days of T_{max}>34°C ranging
294 from an average 10 at S1 to 20 at S8. Under the Dry scenario, the number of days of
295 T_{max}>34°C increased at all the locations, with two location showing evident changes with
296 respect to the others. At Italy-Fiorenzuola, the number of days T_{max}>34°C changed from 0 to
297 an average of 2.5, and at Jordan-Rabba they increased from an average of 5.5 to 18 days (Fig.
298 4). At the latter location, such increase is more evident for later planting time; while in Syria-
299 Breda where at S8 there was an increase of 10 days with respect to the baseline (Fig. 4). The
300 number of days of T_{max}>34°C under the Wet scenario was still high but slightly lower than
301 the Dry one. For example, in Syria-Breda, the number of days T_{max}>34°C at S8 was on
302 average 22, 28, and 25 under the Baseline, Dry, and Wet, respectively (Fig. 4). However, at
303 Jordan-Rabba such variable increased by 15% across all the sowing dates with evident
304 changes at S7 and S8 where the number of days of T_{max}>34°C was 27 and 30, respectively
305 (Fig. 4).

306 The cumulative rainfall from the start of simulation to planting to anthesis and to maturity is
307 shown in Figure 5. At Sowing, the cumulative amount increased from the early to the later
308 sowing dates for each location and each scenario. However, the cumulated amount at anthesis
309 did not show such difference. At Jordan-Rabba, there was more rainfall at planting for the

later sowing dates across all the different scenarios. At the same location, the cumulative rainfall at anthesis was on average of 347, 232, and 417 mm for the baseline, Dry and Wet scenarios, respectively (Fig. 5). At maturity, there was only an additional 5, 5, and 7 mm of rainfall added under the baseline, Dry, and Wet scenario. On the other hand, in the same country but at different location (Jordan-Ramtha), there was lower cumulated rainfall at anthesis, with 235mm for the baseline, 175mm for the Dry scenario, and 291mm for the Wet scenario (Fig. 5). The inter-annual variability, expressed by the boxes' length, was higher for Italy-Fiorenzuola, Algeria, and Italy-Foggia, but for all the other locations, the inter-annual variability of cumulative rainfall was lower. The number of rainy days was higher for the vegetative stage, but it decreased for later sowing dates (Fig. A7).

The cumulative amount of rainfall that fell between summer and sowing determine the amount of water stored in the soil. Such information is plotted in Figure 6 and calculated using equation [5]. The flat lines represent the initial extractable soil water content in summer, when crop simulation was started. The negative values indicated that there was more water at the start of the simulation with respect to a point in time. It does not show the dynamic, but from the simulated daily soil extractable water content key points in time were selected (Fig. S8). The initial conditions of soil water slightly differ among locations due to the information used as initial values from the work of Francia et al. (2011). At sowing, across all the locations and sowing dates there was a range of extractable water of -70 and 174mm for the baseline, -70 to 159mm for the Dry scenario, and -72 and 186mm for the Wet Scenario (Fig. 6). At anthesis, the extractable water content ranged between values of -81 to 126mm, -75 to 92, and -72 to 125mm for the baseline, Dry and Wet scenarios, respectively (Fig. 6). In addition, such values decreased further at maturity ranging between -81 to 28mm for the baseline, -80 to 7mm for the Dry scenario and -83 to 54mm for the Wet scenario. At sowing, there was a strong effect of the sowing dates, with the S5 to S8 showing the higher

amount of extractable water content (Fig. 6). For Italy-Fiorenzuola, from S3 to S8 the extractable soil water content was higher than the initial one; but, similar patterns were found for Italy-Foggia, and Syria-Tel Hadya. At this latter location, however, the impact of later sowing dates on the extractable soil water content was evident. In fact, at planting date S1 the average extractable soil water was -17mm with a very narrow inter-annual variability, at anthesis it was 10mm, with some year having -40mm and other years reaching 50mm (Fig. 6). On the other hand, at planting date S8 there was an average of 70 mm with some years showing extractable soil water of 134mm. However, by anthesis, the average soil water content was -17mm, and even the year with the high extractable soil water showed a -13 mm of extractable water (Fig. 6). There was a high inter-annual variability at planting for extractable soil water content, it was mirroring the amount of cumulated rainfall (Fig. 5); but it was sowing date- and location-specific.

At Jordan-Rabba, the Wet scenario results showed negative yield changes at each sowing date (Fig. 2). At this specific location there was a high number of days of T_{max}>34°C which were negatively related to simulated yield (Fig. 7a). At anthesis, for the Wet scenarios, there was up to 400 mm of cumulated rainfall, but the simulated yield was only 2200 kg DM ha^{-1} and there was no yield increase beyond 300 mm of rainfall cumulated at anthesis (Fig. 7b). A similar relationship was observed between rain, grain yield and the Δ-extractable soil water content at anthesis (Fig. S9). There was also a linear negative relationship between Δ extractable soil water content at anthesis and number of days of T_{max}>34°C (Fig. 7c). In fact, for the Dry scenario at 26 days of T_{max}>34°C there was the maximum Δ of extractable soil water content of -65mm (Fig. 7c). The relationship between Δ extractable soil water content at anthesis and cumulative rainfall at anthesis was linear, with high rainfall corresponding to lower Δ extractable soil water content at anthesis (Fig. 7d).

The variation due to inter-annual weather patterns was the component that carried most of the variability at each of the locations, ranging from 19 to 100% (Fig. 8). The different scenarios also showed higher variability, ranging from 5 to 79% across locations. The variability given by sowing dates under future conditions was lower than the ones under baseline conditions, probably due to the impact of the different scenarios used. Some locations showed higher variability than others, especially Jordan-Ramtha, Jordan-Rabba and Spain, where the inter-annual variability ranged between 77 to 100% (Fig. 8). At those location, the future scenarios also had higher variability with values ranging from 52 to 79%. In Italy-Foggia, the variability due to the scenarios was slightly higher than the inter-annual variability and in Italy-Fiorenzuola, except the inter-annual variability, all the other factors did not show higher values of variability (Fig. 8).

4. Discussion

Different climate projections showed contrasting impacts of simulated barley yield at each location across the Mediterranean environment due to rainfall and temperature changes. At some location (e.g. Italy), the impact of extractable soil water content was more relevant than the heat stress, while in others the number (e.g. Jordan) of days of T_{max}>34°C caused significant yield decrease. Agronomic adaptations, such as shifting sowing dates minimize the negative impacts of climate change. The inter-annual weather variability impacts barley yield irrespective of the sowing dates and the future projected climate.

The results of the barley model evaluation are in line with the ones reported in other studies where the coefficient of determination for simulated yield was 0.88 (Trnka e al., 2004); Al-Bakri et al. (2010) reported values of RMSE for simulated yields of 586 kg DM ha^{-1}, while values ranging between 292 and 720 kg DM ha^{-1} were reported in Fatemi et al. (2014).

383 The simulation of barley phenology was also in line with RMSE for heading of 5.6 days
384 reported by Travasso and Magrin (1998). In this study, the RMSE for the simulated yield at
385 evaluation was slightly higher, but this is due by three experiments in Jordan having observed
386 yields of 70, 500, and 800 kg DM ha^{-1}, which caused an overestimation of yield at such
387 locations. The reason for some other lack of fit between observed and simulated data was
388 because at some locations it was observed a severe frost impact (e.g. in Fiorenzuola), while in
389 others, there was a poor canopy vigour leading to lower observed yields. The crop model was
390 set up for running in conditions of good establishment and any damages other than heat and
391 drought are currently not considered. Table A4 showed the reasons why some simulated
392 yields could not reproduce the observed values (frost or poor canopy vigour), but in one case,
393 JORB there were no indications on why 70 kg DM ha^{-1} were observed. Due to the length of
394 time passed from that field experiment there was no record of what really happened. It was
395 decided to keep it for the sake of clarity.

396 The gap-filling process using the AgMERRA dataset was made only after comparing the
397 observed dataset available with the downloaded data. Overall, the results are in line with the
398 reported outputs from Ruane et al. (2015) indicating the suitability of using the AgMERRA
399 product for the baseline period (1980-2010). Such dataset has been used in numerous studies
400 of climate change impacts as baseline period, allowing meaningful comparisons of climate
401 impacts during the 1980-2010 period (Xie et al., 2018; Asseng et al., 2013; 2015; 2016;
402 Rosenzweig et al., 2014; Elliot et al., 2015). In the current study, some locations (e.g.
403 Turkey) showed an over-estimation of solar radiation by AgMERRA and an under-estimation
404 of minimum and maximum temperature (Figs. A1-A3). On the other hand, locations like
405 Syria-Breda and Jordan-Ramtha showed the opposite behaviour. Such bias could impact the
406 simulated yield because an overestimation of daily temperature means that crops will be
407 subjected to higher than normal temperatures and therefore exacerbate the response to heat

408 stress. However, the over/underestimation of weather variable on the baseline simulation has
409 been quantified to be on average 15% for simulated yield. Taylor et al. (1999) reported that
410 the variation of wheat yields in field experiments is about 13.5%. Therefore, we considered
411 that our bias introduced by the AgMERRA product to be in the range of the observed error.

412 Reported changes in simulated yield in this study were disaggregated by the type of climate
413 scenario used at a given RCP. Overall, the average climate impact on grain yield across the
414 three scenarios was 9%, in line with the 15% reported results in Al-Bakri et al. (2010) for
415 Jordan and with the mean global reduction of 10% reported in Xie et al. (2018). And, it is
416 also in line with experimental results on other cereal crops (wheat) as reported in field
417 experiments (Ottman et al., 2012; Asseng et al., 2015). The simulation study of Al-Barki et
418 al. (2010) could be used as benchmark against our simulated results in Jordan. However, their
419 results were obtained by adding incremental changes of either rainfall or temperature. As a
420 result, they could evaluate the sensitivity of rainfall changes at a given temperature level (e.g.
421 keeping temperature constant but varying rainfall). In this study, the dynamic changes of
422 temperature and rainfall were analysed together because they will most likely act as a system.
423 In fact, results of this study showed that under the Dry scenario the mean growing season
424 temperature tends to be slightly higher than the one under the Wet scenarios, which is likely
425 to be caused by more radiation under a Dry scenario than under a cloudy Wet scenario.

426 There was an interaction between the amount of rainfall, the extractable soil water content
427 and the maximum air temperature as evident in Jordan-Rabba. In that location at higher
428 maximum temperatures there was less extractable soil water and lower yields. However, the
429 impact of the different amount of rainfall and heat differs among locations in the same
430 country. For example, in Jordan the Wet scenarios showed contrasting results at the two
431 locations. Both Rabba and Ramtha had clay soils, with similar plant available water content;
432 at Jordan-Ramtha there was on average 137 mm of available soil water content for the soil

depth, while at Jordan-Rabba was 142 mm (Tab. A2). However, Jordan-Rabba had higher number of days of T_{max}>34°C and even if it had a higher extractable soil water content it did not counteract the impact of higher temperatures. The high number of days of T_{max}>34°C caused higher soil water depletion from the plant and therefore lower yields under the wet scenario. In addition, Asseng et al., (2011) concluded that daily maximum temperatures above 34°C means that leaf senescence rates are accelerated 3-folds, and such higher temperature has also a negative impact of grain filling rates and grain abortion rates (Fisher, 1980). Liu et al. (2016) compared simulated and observed data of the impacts of heat stress at anthesis and grain filling stages. They found that for every unit increase of heat degree-days grain yield was reduced by 1.0–1.6%. The CERES-Wheat model used in this study has also been evaluated in many locations across Asia, Europe, and America encompassing a variety of pedo-climatic conditions (Koo and Rivington, 2005. Timsina & Humphreys, 2006). Crop growth is directly related to the amount of soil water/rainfall, solar radiation, and nutrient availability to the crop. These factors are interrelated, because while roots are responsible to uptake water and nutrients the canopy is responsible for capturing solar radiation and CO_2 - and then transform these into biomass (Jamieson and Ewert, 1998; Sadras and Angus, 2006). Therefore, the results of this study are an attempt to start considering the whole system together where the impact of temperature is not considered *per-se*, but it is also analysed as function of the location-specific soil characteristics. By running the crop simulation model from the summer prior sowing this study accounted also the water stored prior sowing which in such environments is an important determinant of grain yield as found in other studies (Basso et al., 2010, 2011, 2012; Sadras, 2002; Sadras et al., 2012). The overall amount of stored water in the soil over the winter period would also help to minimize the impact of the inter-annual variability on grain yield under current and future climate projections. This was evident in some locations like Foggia (Italy) were simulated yields responded positively to

the Wet scenario and for the late sowing dates. In that location, the number of days of Tmax>34°C is similar for the Dry and Wet scenarios but simulated yields were higher for the Wet than the Dry scenario (Figure 2). Figure 6 showed that for the Wet scenario Foggia held higher extractable water content for later sowing dates as a result of accumulation of stored water. This means that respect to the earlier sowing dates, later sowing will take advantage of more stored water to help their growth, especially in the earlier phases.

To preserve the soil water content and improving grain yield, farmers will need to adopt different sustainable agronomic practices. On the one hand, the shifting of sowing dates is a viable adaptation option for escaping terminal drought in this environment. Another agronomic practice that was not considered in this study, aimed at increasing soil water content is through the improvement of the soil organic carbon (Rawls et al., 2003). Anjum et al. (2011) studying maize (*Zea mays* L.) suggested that, exogenous applications of fulvic acid substantially ameliorated the adversities of drought increasing canopy chlorophyll. These beneficial effects might be tested also on barley when cropped in the Mediterranean basin.

Ceccarelli et al. (2000) suggested that along with agronomy, breeding is an important aspect to take into consideration. Timing and duration of reproductive stages are two important factors affecting breeding strategies. In fact, matching the crop development to the environmental resources is one the greatest challenge for achieving higher yields in new genotypes (Ceccarelli et al., 2000). In Mediterranean environments terminal drought is a known problem and results of this study show that it will be exacerbated by climate change. Because of the different nature and intensity of the terminal drought, traits such as root architecture (Richards et al., 2010) or prostrate habit, vigorous seedling growth, good ground cover, early ear emergence, many ears m^{-2} and large grains (Acevedo et al. 1991) may play a different role in different locations.

There are several limitations to this study, the cultivar used is a generic barley variety calibrated in the Mediterranean basin and does not consider genetic differences among cultivars as done in Zheng et al. (2013). Furthermore, it does not consider current and future breeding activities for adaptation that may lead to more resilient barley genotypes. This is particularly relevant for this species, with genotypes locally adapted to a diversity of potential extreme growing conditions. In addition, the model does not use canopy temperatures in the simulations. The canopy temperature can be cooler than the air temperature by several degrees during transpiration due to evaporative cooling (Kumar & Tripathi, 1991) or can be warmer by several degrees in situations where there is no soil water available for transpiration (Fischer, 1980). Although important for such kind of studies there is a recent scientific effort to understand the best modelling approach for considering canopy temperature impacts (Webber et al., 2017;2018).

5. Conclusions

The impact of future climate on barley yield in the Mediterranean is negative. Such impact differs among locations, with some areas being worse off than others are. However, the negative impact of climate change depends on the climate projection considered, as some of the GCMs showed an increase in growing season rainfall. The increase in rainfall does not always translates into higher yields because the number of days of T_{max}>34°C at reproductive stage offsets such gains. The current sowing window across the Mediterranean basin (Sep-Dec) will still be relevant under future conditions, linking climate forecasts systems with crop simulation models could help to refine the sowing window for each growing season.

506 **Acknowledgments**

507 Prof. A. Suleiman for kindly providing soil information at the locations in Jordan. We also
508 thank the referees for the valuable comments and suggestions that helped to improve the
509 manuscript.

510

511 **References**

512 Acevedo E., Craufurd P.Q., Austin R.B., Perez-Marco P. (1991). Traits associated with high
513 yield in barley in low-rainfall environments. The Journal of Agricultural Science, 116(1),
514 23-36.

515 Al-Bakri J., Suleiman A., Abdulla F., Ayad J. (2010). Potential impact of climate change on
516 rainfed agriculture of a semi-arid basin in Jordan. Physics and Chemistry of the Earth, 35,
517 125-134.

518 Anjum, S.A., Wang L., Farooq M., Xue L., Ali S. (2011). Fulvic acid application improves
519 the maize performance under well-watered and drought conditions. Journal of Agronomy
520 and Crop Science, 197(6), 409-417.

521 Asseng S., Cammarano D., Basso B., Chung U., Alderman P.D., Sonder K., Reynolds M.,
522 Lobell D.B. (2016). Hot spots of wheat yield decline with rising temperatures. Global
523 Change Biololgy. doy: 10.1111/gcb.12530

524 Asseng S., Ewert F., Martre P., et al. (2015). Rising temperatures reduce global wheat
525 production. Nature Climate Change, 5, 143–147.

526 Asseng S., Ewert F., Rosenzweig C., Jone, J.W., Hatfield J.L., Ruane A.C., Boote K.J.,
527 Thorburn P.J., Rotter R.P., Cammarano D., Brisson N., et al. (2013). Uncertainty in
528 simulating wheat yields under climate change. Nature Climate Change. doi:
529 10.1038/nclimate1916.

530 Asseng S., Foster I., Turner N.C. (2011). The impact of temperature variability on wheat
531 yields. Global Change Biology, 17, 997–1012.
532 Basso B., Cammarano D., Troccoli A., Chen D., Ritchie J.T. (2010). Long term wheat
533 response to nitrogen in a rainfed Mediterranean environment: Field data and simulation
534 analysis. European Journal of Agronomy, 33, 132–138.
535 Basso B., Fiorentino C., Cammarano D., Cafiero G., Dardanelli J. (2012). Analysis of rainfall
536 distribution on spatial and temporal patterns of wheat yield in Mediterranean environment.
537 European Journal of Agronomy, 41, 52-65.
538 Basso B., Ritchie J.T., Cammarano D., Sartori L. (2011). A strategic and tactical management
539 approach to select optimal N fertilizer rates for wheat in a spatially variable field. European
540 Journal of Agronomy, 35, 215–222.
541 Brisson N., Gate P., Gouache D., Charmet G., Oury F.X., Huard F. (2010). Why are wheat
542 yields stagnating in Europe? A comprehensive data analysis for France. Field Crop
543 Research, 119, 201-212.
544 Cammarano D., Tian D. (2018). The effects of projected climate and climate extremes on a
545 winter and summer crop in the southeast USA, Agricultural and Forest Meteorology, 248:
546 109–118.
547 Challinor, A.J., Watson J., Lobell D.B., Howden S.M., Smith D.R., Chhetri N. (2014). A
548 meta-analysis of crop yield under climate change and adaptation. Nature Climate Change, 4,
549 287–291.
550 CLIMsystems Ltd, New Zealand, www.climsystems.com (verified October 2018).
551 Ceccarelli S., Grando S., Tutwiler R., Baha J., Martini A., Salahieh H., Goodchild A.,
552 Micheal M. (2000). A methodological study on participatory breeding I. Selection phase.
553 Euphytica, 111, 91-104.

554 Ceccarelli S., Grando S., Capettini F. (2011). Barley Breeding History, Progress, Objectives,
555 and Technology, Near East, North and East Africa and Latin America. In: S.E. Ullrich (ed.),
556 Barley: Production, Improvement and Uses, Wiley-Blackwell, Ames (Iowa), USA, 210-
557 220.
558 Dawson I.K., Russel J., Powell W., Steffenson B., Thomas W.T.B., Waugh R. (2015).
559 Barley: a translational model for adaptation to climate change. New Phytologist, doi:
560 10.111/nhp. 13266
561 Elliott J., Muller C., Deryng D., Chryssanthacopoulos J., Boote K.J., Buchner M., Foster I.,
562 Glotter M., et al. (2015) The global gridded crop model intercomparison: data and modeling
563 protocols for phase 1 (v1.0). Geoscientific Model Development. doi: 10.5194/gmd-8-261-
564 2015
565 FAOSTAT, 2018. Food and Agriculture Organization of the United Nations, Viale delle
566 Terme di Caracalla, 00153 Rome, Italy (http://www.fao.org/faostat/en/#home; accessed
567 Nov 2018).
568 Fatemi Z., Pknejad F., Amiri E., Eilkaee M.N. (2014). Capability of the CERES-Barley
569 Model for Prediction of Barley Varieties Growth under Deficit Irrigation. Journal of
570 Biology, 2, 1-7.
571 Fischer R.A. (1980) Influence of water stress on crop yield in semiarid regions.
572 In: Adaptation of Plants to Water and High Temperature Stress (eds Turner NC, Kramer
573 PJ), pp. 323–339. Wiley, New York.
574 Francia E., Tondelli A., Rizza F., Badeck F.W., et al. (2011). Determinats of bazrely grain
575 yield in a wide range of Mediterranean environments. Field Crop Research, 120, 169-178.
576 Grando S., Gormez Macpherson H. (eds.) (2005) Food Barley: Importance, Uses and Local
577 Knowledge. Proceedings of the International Workshop on Food Barley Improvement, 14-
578 17 January 2002, Hammamet, Tunisia. ICARDA, Aleppo, Syria, x+156 pp.

579 Hoogenboom G., Jones J.W., Wilkens P.W., Porter C.H., et al. (2010). Decision Support
580 System for Agrotechnology Transfer (DSSAT), Version 4.5 (CD-ROM). University of
581 Hawaii, Honolulu, HI.
582 Huntingford C., Hugo Lambert F., Gash J.H.C., Taylor C.M., Challinor A.J. (2005). Aspects
583 of climate change prediction relevant to crop productivity. Philosophical Transactions of the
584 Royal Society B: Biological Sciences, 360, 1999–2009.
585 Jamieson P.D., Ewert F. (1999). The role of roots in controlling soil water extraction during
586 drought: an analysis by simulation. Field Crop Research, 60, 267-280.
587 Jones J.W., Hoogenboom G., Porter C.H., Boote K.J., et al. (2003). The DSSAT cropping
588 system model. European Journal of Agronomy, 18, 235–265.
589 Kobza J., Edwards G.E. (1987). Influences of leaf temperature on photosynthetic carbon
590 metabolism in wheat. Plant Physiology, 83, 69–74.
591 Koo J., Rivington M. (2005). Report on the Meta-analysis of Crop modelling for Climate
592 Change and Food Security Survey Climate Change. Agriculture and Food Security
593 (CCAFS), Challenge Program, Denmark.
594 Kumar A., Tripathi R.P. (1991). Relationships between Leaf Water Potential, Canopy
595 Temperature and Transpiration in Irrigated and Non-irrigated Wheat. Journal of Agronomy
596 and Crop Science, 166, 19-23.
597 Liu B., Asseng S., Muller C., Ewert F., Elliot J., et al. (2016). Similar estimates of
598 temperature impacts on global wheat yield by three independent methods. Nature Climate
599 Change. doi: 10.1038/nclimate3115.
600 Lobell D.B., Burke M.B., Tebaldi C., Mastrandrea M.D., Falcon W.P., Naylor R.L. (2008).
601 Prioritizing climate change adaptation needs for food security in 2030. Science, 319, 607–
602 610.

603 Martre P., He J., Le Gouis J., Semenov M.A. (2015). In silico system analysis of
604 physiological traits determining grain yield and protein concentration for wheat as
605 influenced by climate and crop management. Journal of Experimental Botany, 66, 3581–
606 3598.
607 O'Leary G.J., Christy B., Nuttal J., Huth N., Cammarano D., et al. (2015). Response of wheat
608 growth, grain yield and water use to elevated CO_2 under a Free-Air CO_2 Enrichment
609 (FACE) experiment and modelling in a semi-arid environment. Global Change Biology, 21,
610 2670–2686.
611 Ottman M.J., Kimball B.A., White J.W., Wall G.W. (2012) Wheat growth response to
612 increased temperature from varied planting dates and supplemental infrared heating.
613 Agronomy Journal, 104, 7–16.
614 Passioura J., 2006. Increasing crop productivity when water is scarce—from breeding to field
615 management. Agricultural Water Management, 80, 176-196.
616 Porter J.R., Xie L., Challinor A.J., Cochrane K., Howden M., Iqbal M.M., Lobell D.B.,
617 Travasso M.I. (2014). Chapter 7. Food security and food production systems. Climate
618 change 2014: impacts, adaptation and vulnerability. Working Group II Contribution to the
619 IPCC 5th Assessment Report. Geneva, Switzerland.
620 Rawls W.J., Pachepsky, Y.A., Ritchie J.C., Sobecki T.M., Bloodworth H. (2003). Effect of
621 soil organic carbon on soil water retention. Geoderma, 116(1-2), 61-76.
622 Richards R.A., Rebetzke G.J., Watt M., Condon A.G., Spelmeyer W., Dolferus R. (2010).
623 Breeding for improved water productivity in temperate cereals: phenotyping, quantitative
624 trait loci, markers and the selection environment. Functional Plant Biology, 37, 85-97.
625 Rosenzweig C., et al. (2014). Assessing agricultural risks of climate change in the 21st
626 century in a global gridded crop model intercomparison. Proceedings of the National
627 Academy of Sciences of the United States of America, 111, 3268–73.

628 Rosenzweig C., Hillel, D. (Eds.) (2015). Handbook of Climate Change and Agroecosystems:
629 The Agricultural Model Intercomparison and Improvement Project (AgMIP) Integrated
630 Crop and Economic Assessments. ICP Series on Climate Change Impacts, Adaptation, and
631 Mitigation Vol. 3. Imperial College Press, doi:10.1142/p970.
632 Rötter R.P., Palosuo T. Kersebaum K.C., Angulo C., Bindi M., et al. (2012). Simulation of
633 spring barley yield in different climatic zones of Northern and Central Europe: A
634 comparison of nine crop models. Field Crop Research, 133, 23–26.
635 Ruane A.C., Goldberg R., Chryssanthacopoulos J. (2015). Climate forcing datasets for
636 agricultural modeling: merged products for gap-filling and historical climate series
637 estimation Agricultural and Forest Meteorology, 200, 233–48.
638 Ruane A.C., McDermid S.P. (2017). Selection of a representative subset of global climate
639 models that captures the profile of regional changes for integrated climate impacts
640 assessment. Earth Perspectives. doi: 10.1186/s40322-017-0036-4.
641 Sadras V.O. (2002). Interaction between rainfall and nitrogen fertilization of wheat in
642 environments prone to terminal drought: economic and environmental risks analysis. Field
643 Crop Research, 77, 201-215.
644 Sadras V.O., Angus J.F. (2006). Benchmarking water-use efficiency of rainfed wheat in dry
645 environments. Australian Journal of Agricultural Research, 57, 847-856.
646 Sadras V.O., Lawson C., Hooper P., McDonald G. (2012). Contribution of summer rainfall
647 and nitrogen to the yield and water use efficiency of wheat in Mediterranean-type
648 environments of South Australia. European Journal of Agoronomy, 36, 41-54.
649 Saseendran S.A., Ahuja L.R., Timlin D., Stockle C.O., Boote K.J., Hoogenboom G. (2008).
650 Current water deficit stress simulations in selected agricultural system models. In: Response
651 of Crops to Limited Water: Understanding and Modeling Water Stress Effects on Plant

652 Growth (Ahuja L.R., Reddy V.R., Saseendran S.A., Qiang Y., Eds.). Advances in
653 Agricultural Systems Modeling 1. American Society of Agronomy, Inc., WI, USA.
654 Semenov M.A., Stratonovitch P., Alghabari F., Gooding M.J. (2014). Adapting wheat in
655 Europe for climate change. Journal of Cereal Science, 59, 245–256.
656 Senapati N., Stratonovitch P., Paul M.J., Semenov M.A. (2018). Drought tolerance during
657 reproductive development is important for increasing wheat yield potential under climate
658 change in Europe. Journal of Experimental Botany. doi: 10.1093/jxb/ery226
659 Tao F., Rotter R.P., Palosuo T., Diaz-Ambrona C.G.H., Ines Mingues M., et al. (2018).
660 Contribution of crop model structure, parameters and climate projections to uncertainties in
661 climate change impact assessments. Global Change Biology, doi: 10.1111/gcb.14019
662 Taylor, S.L., Payton, M.E., Raun, W.R. (1999). Relationship between mean yield, coefficient
663 of variation, mean square error, and plot size in wheat field experiments. Communication in
664 Soil Science and Plant Analysis, 30, 1439–1447.
665 Taylor K.E., Stouffer R.J., Meehl G.A. (2012). An Overview of CMIP5 and the experiment
666 design. Bulletin of the American Meteorological Society, 93, 485-498.
667 Timsina J., Humphreys E. (2006). Performance of CERES-rice and CERES-wheat models in
668 rice-wheat systems: a review. Agricultural Systems, 90, 5-31
669 Travasso M.I., Magrin G.O. (1998). Utility of CERES-Barely under Argentine conditions.
670 Field Crop Research, 57, 329-333.
671 Trnka M., Dubrovsky M., Zalud, Z. (2004). Climate change impacts and adaptation strategies
672 in spring barley production in the Czech Republic. Climatic Change, 64, 227-255.
673 Webber H., Martre P., Asseng S., Kimball B., White J., Ottman M., et al. (2017). Canopy
674 temperature for simulation of heat stress in irrigated wheat in a semi-arid environment: A
675 multi-model comparison. Field Crop Research, 202, 21-35.

Webber H., White J.W., Kimball B.A., Ewert F., Asseng S., Rezaei E.E., et al. (2018). Canopy temperature for simulation of heat stress in irrigated wheat in a semi-arid environment: A multi-model comparison. Field Crop Research, 216, 75-88.

Wickham, H (2016). ggplot2: Elegant Graphics for Data Analysis. Springer-Verlag New York, 2016.

Wilmott C.J. (1982). Some comments on the evaluation of model performance. Bulletin American Meteorological Society, 63, 1309–1313.

Xie W., Xiong W., Pan J., Ali T., Cui Q., Guan D., Meng J., Mueller N.D., Lin E., Davis S.J. (2018). Decreases in global beer supply due to extreme drought and heat. Nature Plants. doi.org/10.1038/s41477-018-0263-1

Yin, C., Li, Y., Urich, P., 2013. SimCLIM 2013 Data Manual. CLIMsystems Ltd, New Zealand (available at www.climsystems.com).

Zheng B., Biddulph B., Li D., Kuchel H., Chapman S. (2013). Quantification of the effects of VRN1 and Ppd-D1 to predict spring wheat (Triticum aestivum) heading time across diverse environments. Journal of Experimental Botany. doi:10.1093/jxb/ert209

Table 1. Results of the calibration and evaluation of the generic barley cultivar at three irrigated location for calibration and for the remaining locations for the evaluation.

Step	Variable	r^2	RMSE	d-Index
Calibration	*Heading*	0.99	4 *d*	0.99
	Maturity	0.96	9 *d*	0.98
	Yield	0.85	587 kg *DM* ha^{-1}	0.60
Evaluation	*Heading*	0.97	6 *d*	0.99
	Maturity	0.82	10 *d*	0.99
	Yield	0.55	1200 *kg DM* ha^{-1}	0.80

Table 2. List of the three Global Circulation Models (GCMs) selected at each location and their simulated changes of growing season mean temperature and rainfall respect to the baseline.

ID	GCM	Site ID	Growing season rainfall changes *(%)*	Growing season temperature changes *(%)*
DRY	MIROC4H	Algeria	-13.63	17.12
DRY	INMCM4	Italy-Foggia	-18.81	7.61
DRY	INMCM4	Italy-Fiorenzuola	-16.41	11.60
DRY	MIROC4H	Jordan-Ramtha	-23.94	14.09
DRY	MIROC4H	Jordan-Rabba	-31.72	12.21
DRY	GFDL-ESM2M	Spain	-15.22	10.65
DRY	MIROC4H	Syria-Breda	-14.66	13.60
DRY	MIROC4H	Syria-Tel Hadya	-14.33	13.46
DRY	GFDL-ESM2G	Turkey	-20.82	18.36
MID	HADCM3	Algeria	1.50	8.83
MID	BBC-CSM1-1	Italy-Foggia	1.14	9.09
MID	CANESM2	Italy-Fiorenzuola	0.24	12.39
MID	BBC-CSM1-1	Jordan-Ramtha	-0.12	10.01
MID	ACESS-1.3	Jordan-Rabba	0.28	7.63
MID	NORESM1-M	Spain	0.45	11.37
MID	GFDL-ESM2M	Syria-Breda	-2.47	8.79
MID	NORESM1-ME	Syria-Tel Hadya	0.93	10.07
MID	GFDL-ESM2M	Turkey	0.24	11.59
WET	BBC-CSM1-1	Algeria	20.98	9.83
WET	HADCM3	Italy-Foggia	10.82	9.02
WET	CNRM-CM5	Italy-Fiorenzuola	16.56	10.96
WET	MPI-ESM-MR	Jordan-Ramtha	24.27	7.15
WET	FGOALS-G2	Jordan-Rabba	20.10	11.71
WET	MIROC4H	Spain	14.59	17.09
WET	INMCM4	Syria-Breda	23.96	7.02
WET	INMCM4	Syria-Tel Hadya	23.67	6.95
WET	CNRM-CM5	Turkey	5.07	12.78

730 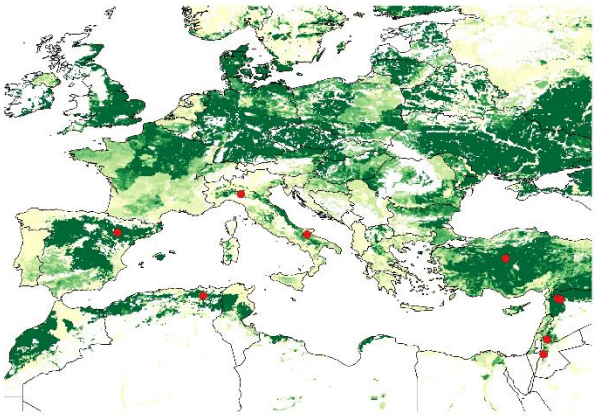

731 **Figure 1.** The red dots indicate the locations of the study of Francia et al. (2011) used in the current
732 work. The green area indicates the barley growing area and the intensity of the cultivation.

733

734

735

736

737

738

739

740

741

742

743

744

745

746

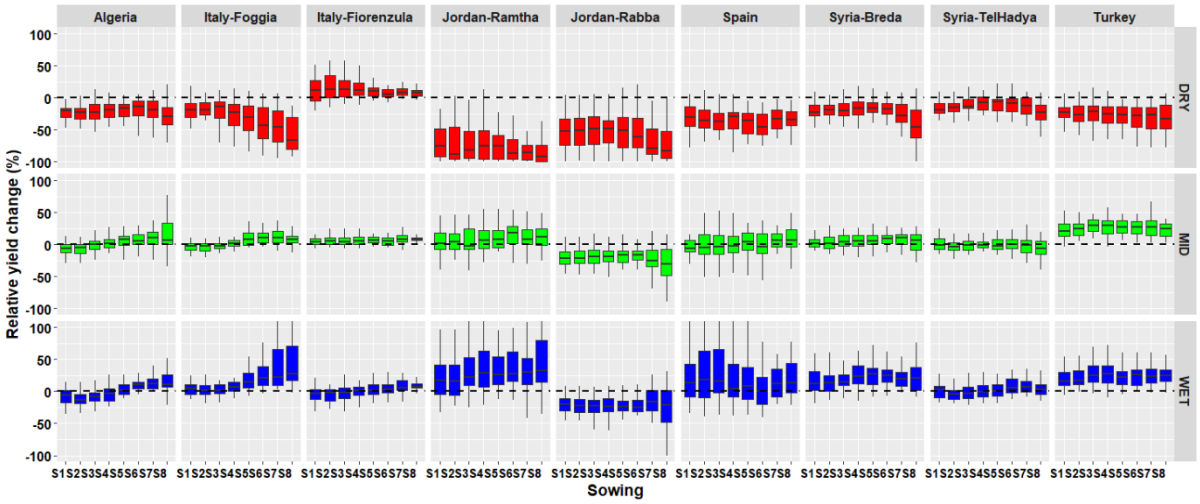

747

748 **Figure 2.** Simulated relative grain yield change for the eight sowing dates and for the "Dry"
749 (red boxplots), "Mid" (green boxplots), and "Wet" (blue boxplots) scenarios. For each
750 boxplot, the end of the vertical line represents, from top to the bottom, the 10th percentile and
751 the 90th percentile. The horizontal line of the box, from the top to the bottom represents the
752 25th, median, and 75th percentile, respectively.

753

754

755

756

757

758

759

760

761

762

763

764

765

766

767

768

769

770

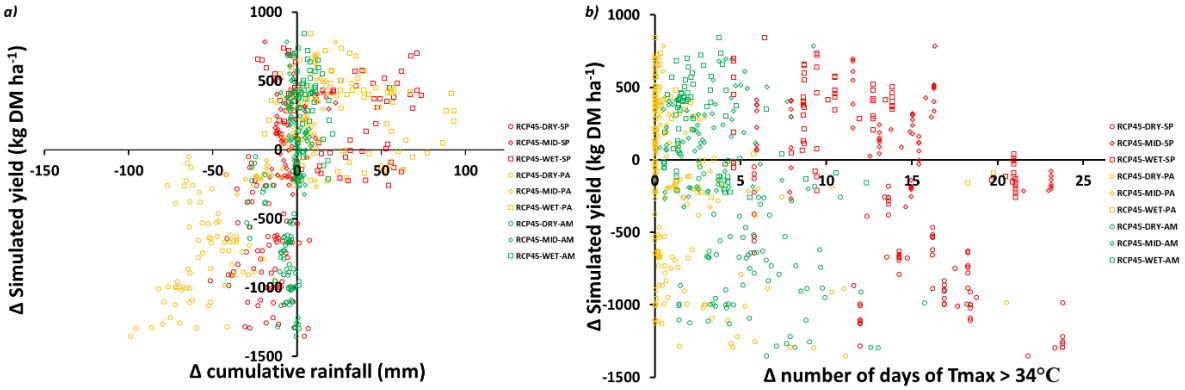

Figure 3. Relationship between Δ simulated grain yield and (***a***) Δ cumulative rainfall and (***b***) number of days of T_{max}>34°C. The three different GCMs were reported in symbols' shape, with circle being the "Dry", diamond being the "Mid", and square being the "Wet". The different stages were reported with different colour-code, start of simulation to sowing (SP, red), sowing to anthesis (PA, yellow), and anthesis to maturity (AM, green).

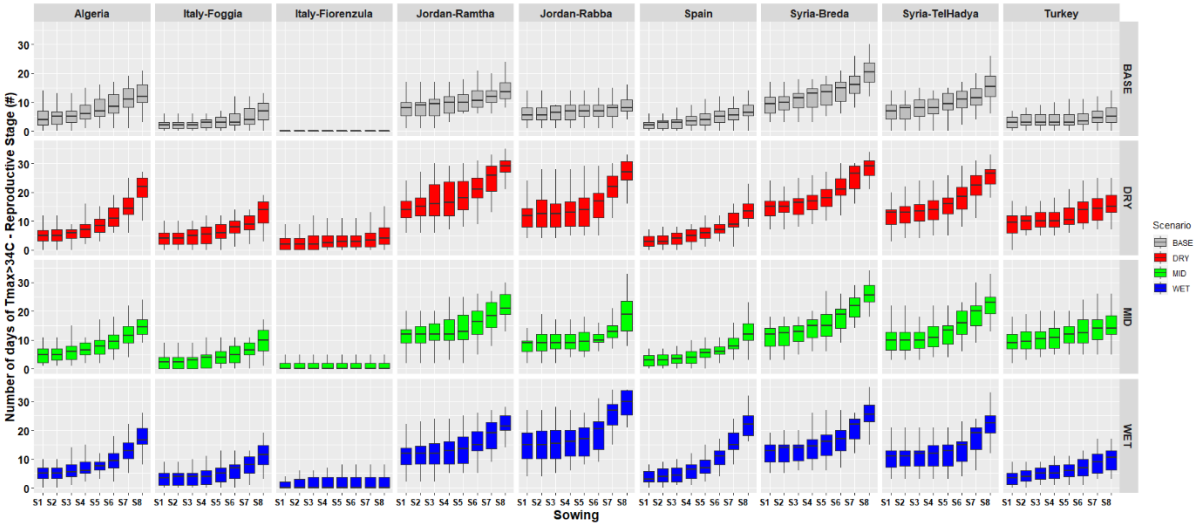

Figure 4. Number of days of T_{max}>34°C at the reproductive stage for the eight sowing dates and for the Baseline (grey boxplots), "Dry" (red boxplots), "Mid" (green boxplots), and "Wet" (blue boxplots) scenarios. For each boxplot, the end of the vertical line represents, from top to the bottom, the 10th percentile and the 90th percentile. The horizontal line of the box, from the top to the bottom represents the 25th, median, and 75th percentile, respectively.

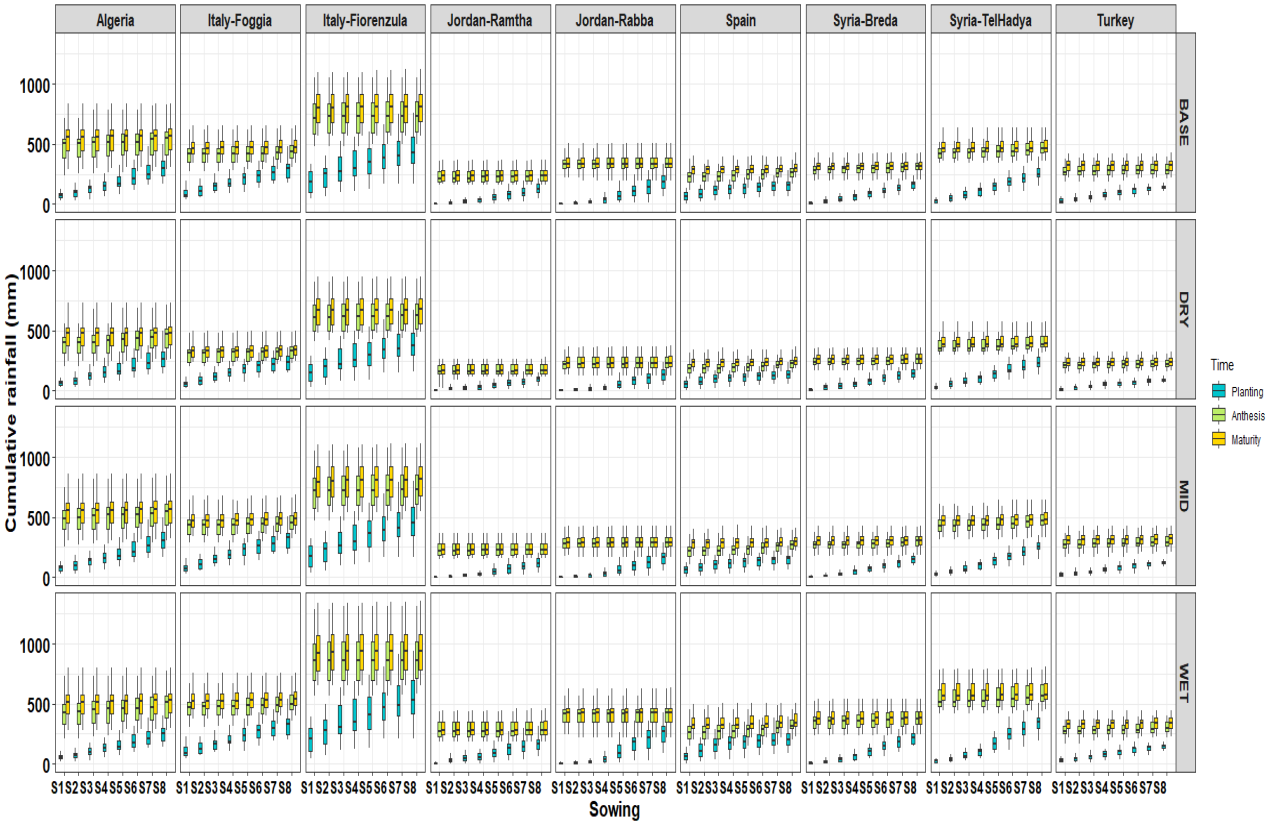

Figure 5. Cumulative growing season rainfall at sowing (blue box), at anthesis (green box) and at maturity (yellow box) for the baseline, "Dry", "Mid", and "Wet" scenarios. For each boxplot, the end of the vertical line represents, from top to the bottom, the 10th percentile and the 90th percentile. The horizontal line of the box, from the top to the bottom represents the 25th, median, and 75th percentile, respectively.

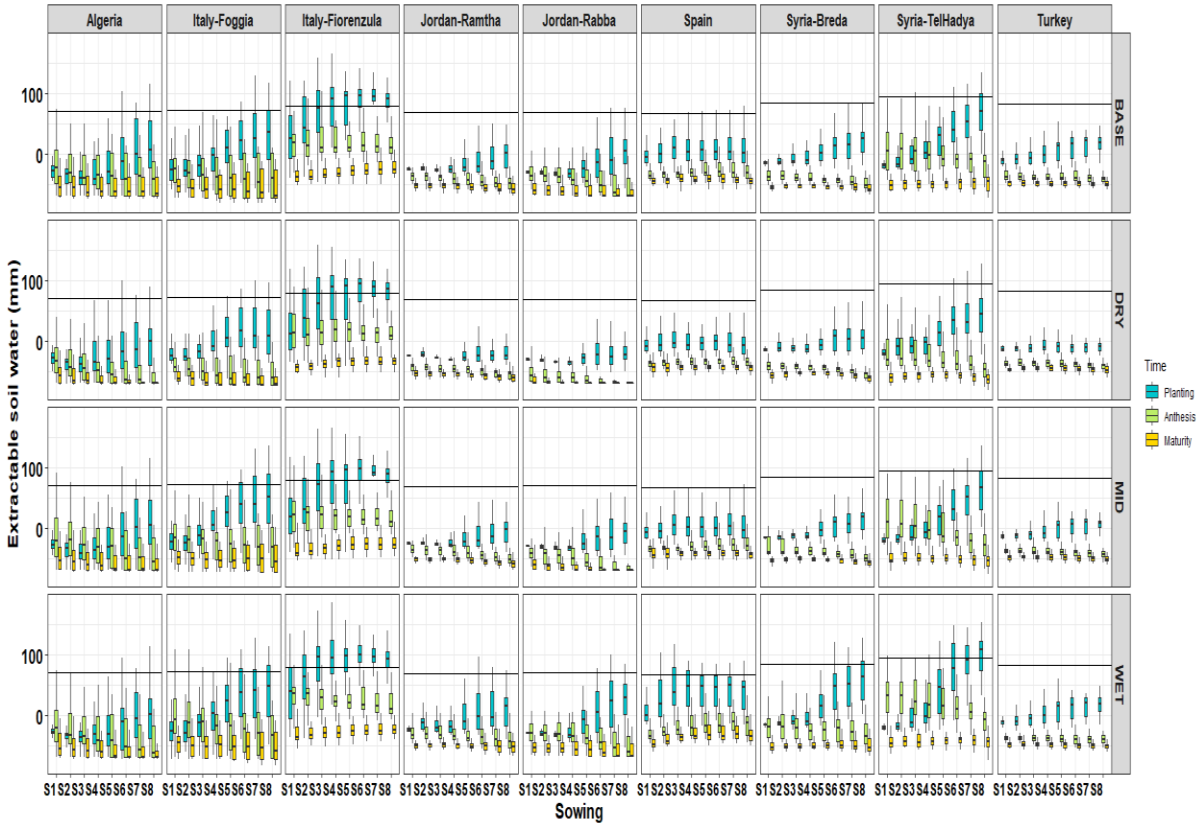

840

841 **Figure 6.** Extractable soil water content at the start of the simulation (full horizontal line), at
842 sowing (blue box), at anthesis (green box) and at maturity (yellow box) for the baseline,
843 "Dry", "Mid", and "Wet" scenarios. For each boxplot, the end of the vertical line represents,
844 from top to the bottom, the 10th percentile and the 90th percentile. The horizontal line of the
845 box, from the top to the bottom represents the 25th, median, and 75th percentile, respectively.

846

847

848

849

850

851

852

853

854

855

856

857

858

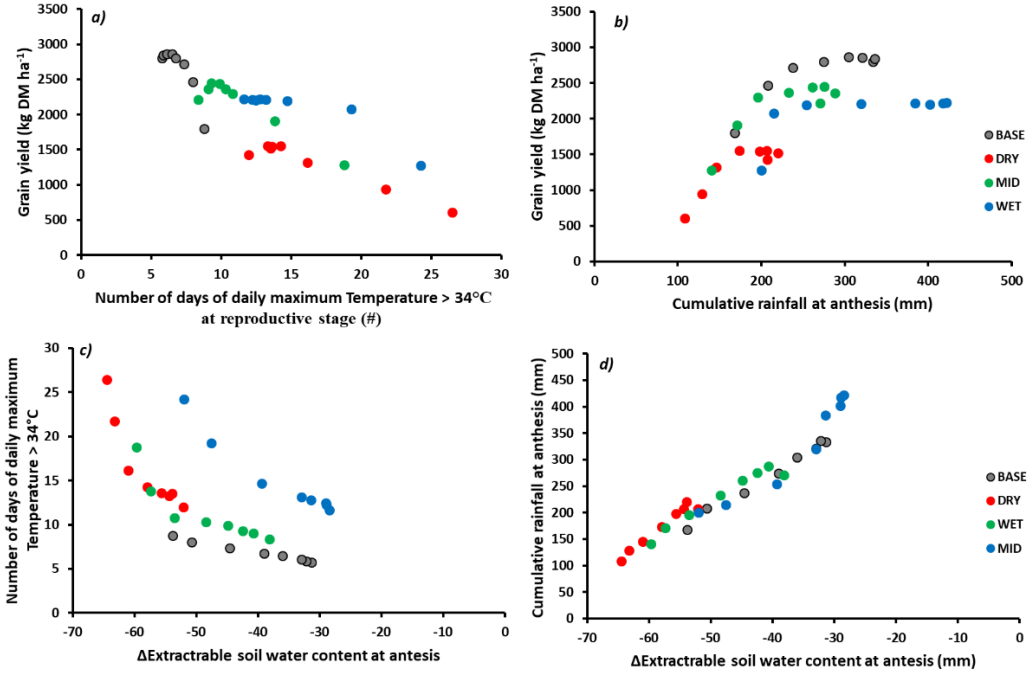

Figure 7. Relationship between (***a***) number of days of T_{max}>34°C at reproductive stage and simulated grain yield; (***b***) cumulative rainfall at anthesis and grain yield; (***c***) Δextractable soil water content at anthesis and number of days of T_{max}>34°C at reproductive stage; and (***d***) Δextractable soil water content at anthesis and cumulative rainfall at anthesis for the baseline (grey dots), Dry (red dots), Mid (green dots), and Wet (blue dots) scenarios at Jordan-Rabba.

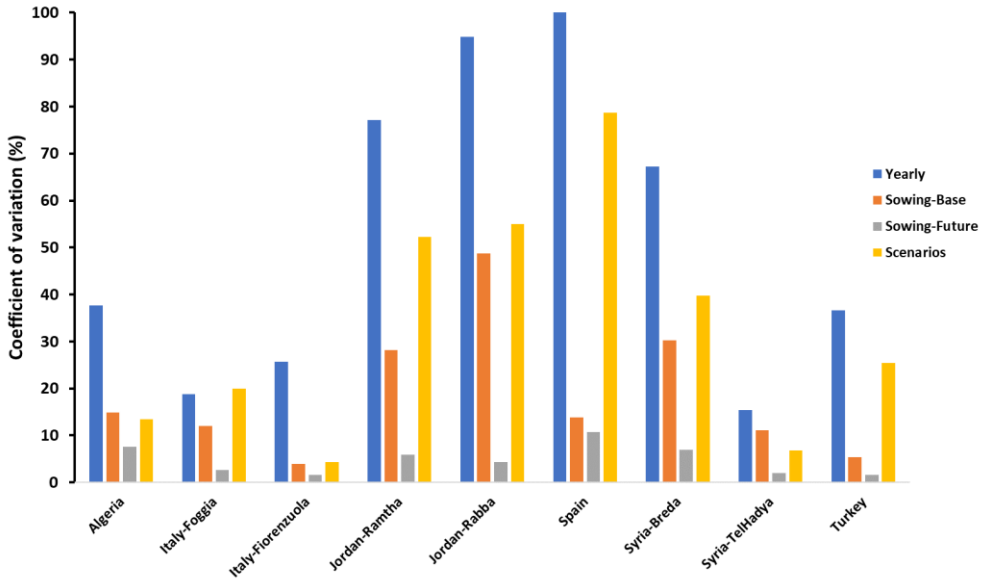

Figure 8. Coefficient of variation due to the inter-annual variation (Yearly; blue bars), the sowing dates under the baseline conditions (Sowing-Base; orange bars), the sowing dates under future conditions (Sowing-Future; grey bars); and the different scenarios used (Scenarios; yellow bars).